# Detection Performance Improvement of FMCW Radar Using Frequency Shift

Yan Wu
Department of Electrical Engineering
Technische Universiteit Eindhoven
y.w.wu@tue.nl

J.P.M.G. Linnartz
Department of Electrical Engineering
Technische Universiteit Eindhoven
j.p.linnartz@tue.nl

**Abstract**

Frequency modulated continuous wave (FMCW) radars have been widely used for measuring target range and speed. In this paper, we present a mathematical model that quantifies the system-level performance of FMCW radar systems. In FMCW radar, the target range is measured through measuring the beat frequency between the transmitted and received signal, usually by using Fast Fourier Transform (FFT). One drawback of this approach is that when the beat frequency of a target is not on the FFT grid, both the detection probability and the false alarm rate (FAR) performances are degraded. In this paper, we propose a new detector, using frequency shifts, that improves the detection probability for off the grid targets at a cost of a slight increase in FAR.

# 1 Introduction

In Frequency Modulated Continuous Wave (FMCW) radar, the transmit signal is generated by frequency modulating a continuous wave signal. In one sweep of the radar operation, the frequency of the transmit signal varies linearly with time. This kind of signal is also known as the chirp signal. As shown in Figure 1, the transmit signal sweep a frequency of $\Delta f$ in one chirp duration. Due to the propagation delay, the received signal bounced back from a target has a frequency difference, called the beat frequency, compared to the transmit signal. The range of the target is proportional to the beat frequency. Thus, by measuring the beat frequency, the target range can be obtained [1]. Similar to other radar systems, there are two important performance indicators in FMCW radar systems, namely the detection probability and false alarm rate (FAR). The detection probability is the probability of detecting a target when it is present, while the FAR is the probability of declaring a target when there is no target. At an algorithmic level, the performance of different detection algorithms for radar systems is usually gauged in terms of the detection probability for a particular signal to noise ratio (SNR) and a given acceptable FAR. From a system level design on the other hand, the system designer is interested in the performance that can be achieved for a certain radar system with a given set of specifications. We have noticed a lack of models that link the performance at these two levels for FMCW radar systems. In view of this, in this paper, we present a mathematical model that models the system-level detection performance for FMCW radars. To illustrate the use of this model, we present an example of evaluating the system-level radar performance in detecting cars, cyclists and pedestrians in traffic monitoring using a typical 24 GHz frequency modulated continuous wave (FMCW) radar.

In FWCW radar, the target range is measured through measuring the beat frequency, which is usually done using Fast Fourier Transform (FFT) due to its low computational complexity [1]. A well know property of the FFT is that each frequency bin has a sinc-shaped spectrum [2]. When the beat frequency of the target falls between the FFT grids in the middle of frequency bins, the detection performance will be degraded due to two factors. Firstly, the amplitude of the target signal at the FFT output is attenuated, which reduces the SNR and hence also the detection probability.

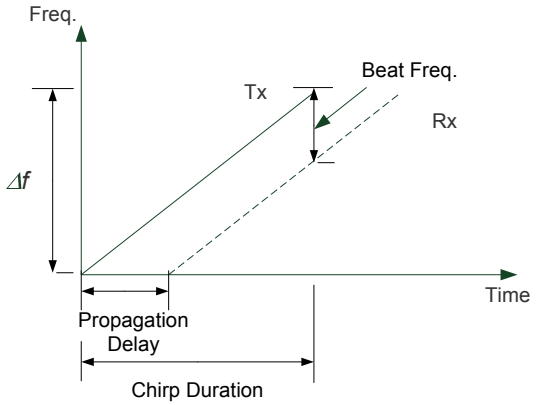


Figure 1: Time-frequency plot of FMCW radar signals.

Secondly, due to the sinc-shaped spectrum, a single target leads to multiple signals present on different FFT grids, which increases the false alarm rate (FAR) in neighboring frequency bins. As a results, the average FAR over all frequency bins is also increased. One popular method to mitigate these degradations is to use windowing before FFT. However, the detector frequency resolution is reduced due to windowing. In this paper, we present a new detector to improve the detection probability for off the FFT grid targets without sacrificing frequency resolution. However, this improvement is achieved at the cost of a slight increase in the average FAR.

# 2 Principles of FMCW radar

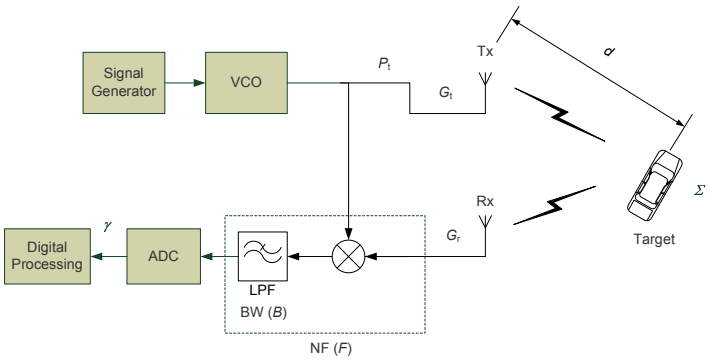


Figure 2: Block diagram of an FMCW radar system.

A block diagram of an FMCW radar system is shown in Figure 2. The transmitter generates a frequency modulated continuous wave using a signal generator and a voltage controlled oscillator (VCO). The transmit signal can be written as

$$x(t) = \sqrt{2P_{\mathrm{t}}} \cos\left(2\pi f_{\mathrm{ca}} t + 2\pi \frac{\Delta f}{2T_{\mathrm{c}}} t^2\right), \tag{1}$$

where $P_{\mathrm{t}}$ is the transmission power, $f_{\mathrm{ca}}$ is the carrier frequency, $\Delta f$ and $T_{\mathrm{c}}$ are the sweep frequency and the chirp duration. The signal is transmitted via the transmit antenna with gain $G_{\mathrm{t}}$ and is reflected back by a target with a radar cross section (RCS) of $\Sigma$ that is $d$ meters away. The received signal from a receive antenna with gain $G_{\mathrm{r}}$

can be written as

$$r(t) = \sqrt{2P_{\mathrm{r}}}\cos\left(2\pi f_{\mathrm{ca}}\left(t-T_{\mathrm{p}}\right)+2\pi\frac{\Delta f}{2T_{\mathrm{c}}}\left(t-T_{\mathrm{p}}\right)^2\right)+n(t), \tag{2}$$

where $P_{\mathrm{r}}$ is the received signal power, $T_{\mathrm{p}}$ is the propagation delay and $n(t)$ is the noise signal. Using the well known radar equation [3], the relationship between $P_{\mathrm{t}}$ and $P_{\mathrm{r}}$ can be expressed as

$$P_{\mathrm{r}} = \frac{P_{\mathrm{t}}G_{\mathrm{t}}G_{\mathrm{r}}\Sigma\lambda^2}{(4\pi)^3 d^4}, \tag{3}$$

where $\lambda$ is the wavelength given by $\lambda = c/f_{\mathrm{ca}}$ with $c = 3\times10^8$ m/s being the speed of light. The received signal is passed through a receiver front end with a certain noise figure (NF) $F$ dB, where it is mixed with transmit LO output and passed through a low pass filter (LPF) with a bandwidth $B$. In FMCW radar, the bandwidth $B$ is determined by $B = \frac{\Delta f 2d_{\max}}{c}\frac{1}{T_c}$, where $d_{\max}$ is the pre-determined maximum distance of targets. The LPF output, which is commonly called the IF signal, can be written by

$$y(t) = \sqrt{2P_y}\cos\left(2\pi\frac{\Delta f}{T_c}T_p t + 2\pi\left(f_{\mathrm{ca}}T_p - \frac{\Delta f}{2T_c}T_p^2\right)\right)+n_y(t), \tag{4}$$

where $P_y$ is the power of the desired signal after LPF and $n_y(t)$ is the noise. The beat frequency $f_{\mathrm{b}}$ is the frequency of the desired signal in $y(t)$, which can be obtained as

$$\begin{aligned} f_{\mathrm{b}} &= \frac{1}{2\pi}\frac{d}{dt}\left(2\pi\frac{\Delta f}{T_c}T_p t + 2\pi\left(f_{\mathrm{ca}}T_p - \frac{\Delta f}{2T_c}T_p^2\right)\right) \\ &= \frac{\Delta f}{T_{\mathrm{c}}}T_{\mathrm{p}} = \frac{\Delta f}{T_{\mathrm{c}}}\frac{2d}{c}. \end{aligned} \tag{5}$$

From (5), we can see that the range of the target $d$ can be obtained straight-forwardly once we know the beat frequency $f_{\mathrm{b}}$. The signal to noise ratio of $y(t)$ is given by $\gamma = \frac{P_y}{P_{n_y}}$. Denoting the front end power gain as $G_{\mathrm{fe}} = P_y/P_{\mathrm{r}}$, $P_y$ can be written as

$$P_y = G_{\mathrm{fe}}P_{\mathrm{r}} = \frac{P_{\mathrm{t}}G_{\mathrm{t}}G_{\mathrm{r}}\Sigma\lambda^2 G_{\mathrm{fe}}}{(4\pi)^3 d^4}. \tag{6}$$

Considering only the thermal noise, the average power of noise $n_y$ can be obtained as

$$\overline{P_{n_y}} = G_{\mathrm{fe}}B10^{(-174-30+F)/10}, \tag{7}$$

where the power spectrum density of the thermal noise is taken as -174 dBm/Hz. Therefore, the average time-domain SNR of the IF signal can be written as

$$\gamma = \frac{\overline{P_y}}{\overline{P_{n_y}}}\frac{P_{\mathrm{t}}G_{\mathrm{t}}G_{\mathrm{r}}\overline{\Sigma}\lambda^2}{(4\pi)^3 d^4 B10^{(-174-30+F)/10}}, \tag{8}$$

where $\overline{\Sigma}$ is the average RCS of the target. The IF signal is then sampled with an analog to digital converted (ADC) and the beat frequency (target range) is estimated using digital processing.

As shown in (5), in the FMCW radar, the range of the target can be estimated through estimating the beat frequency. In practice, the beat frequency is usually estimated using fast fourier transform (FFT) due to its low computational complexity.

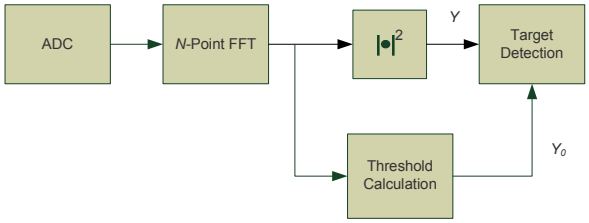


Figure 3: An FMCW detector using FFT.

A common FFT-based FMCW detector is illustrated in Figure 3. Using FFT, the whole bandwidth $B$ is divided into $N$ frequency bins, where $N$ is the FFT size. The FFT output in each frequency bin is passed through a square law detector ($|\bullet|^2$) and the output $Y$ is compared to a calculated threshold $Y_0$ to determine if a target is present. As the target detection is carried out in each frequency bin independently, in the following, we are going to focus on per-bin processing without distinguishing different bins. We consider a Swerling I target model, in which the target RCS stays constant within one radar scan. For different radar scans, the RCS is uncorrelated and follows an exponential distribution as in [3]. As a result, $P_y$ is also exponentially distributed with

$$f(P_y) = \frac{1}{\overline{P_y}} \exp\left(-\frac{P_y}{\overline{P_y}}\right), \tag{9}$$

where $\overline{P_y}$ is the average of $P_y$. Assuming the time-domain thermal noise is circularly symmetric complex Gaussian (CSCG) with an average power given by (7), it can be easily shown that the output of the square law detector $Y$ also follows an exponential distribution given by

$$f(Y) = \frac{1}{\sigma_Y^2} \exp\left(-\frac{Y}{\sigma_Y^2}\right), \quad \text{and } \sigma_Y^2 = \begin{cases} \sigma_n^2; & \text{no target} \\ \sigma_n^2(1+\gamma_{\text{bin}}); & \text{target present.} \end{cases} \tag{10}$$

Here we use $\sigma_n^2$ and $\gamma_{\text{bin}}$ to denote the noise power and the SNR per frequency bin respectively. The bandwidth of a frequency bin, which is also the frequency resolution of the FMCW radar, is given by $1/T_c$ [4]. Therefore,

$$\sigma_n^2 = G_{\text{fe}} \frac{1}{T_c} 10^{(-174-30+F)/10}, \tag{11}$$

and it is related to time-domain noise power $\overline{P_{n_y}}$ by $\overline{P_{n_y}} = N\sigma_n^2$. Similarly, we have

$$\gamma_{\text{bin}} = \frac{\overline{P_y}}{\sigma_n^2} = N\frac{\overline{P_y}}{\overline{P_{n_y}}} = N\gamma. \tag{12}$$

With (10), it can be easily shown that for a constant false alarm rate (CFAR) detector with a desired FAR, the threshold $Y_0$ should be chosen as [5]

$$Y_0 = -\log(\text{FAR})\sigma_n^2,$$

and the detection probability is given by [5]

$$P_{\text{d}} = \exp\left(-\frac{Y_0}{\sigma_n^2(1+\gamma_{\text{bin}})}\right) = \exp\left(-\frac{Y_0}{\sigma_n^2(1+N\gamma)}\right). \tag{13}$$

| Parameter | Value | Parameter | Value |
|---|---|---|---|
| $f_{\mathrm{ca}}$ (GHz) | 24 | $P_{\mathrm{t}}$ (dBm) | 0 |
| $G_{\mathrm{t}}$ (dB) | 18 | $G_{\mathrm{r}}$ (dB) | 18 |
| $F$ (dB) | 15 | BW (kHz) | 64 |
| $T_{\mathrm{c}}$ (ms) | 1 | $N$ | 64 |

Table 1: Specifications of a typical 24 GHz FMCW radar.

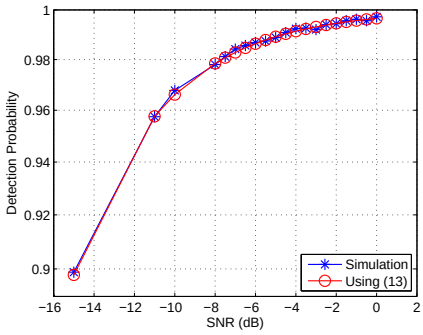


(a) Algorithmic-level performance of the CFAR detector with FAR=0.001.

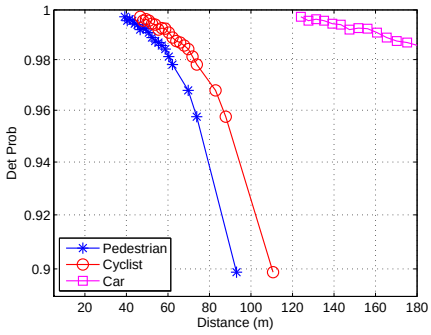


(b) System-level performance for the considered example FMCW radar system for traffic monitoring.

Figure 4: Algorithmic and system-level performance of the example 24 GHz FMCW radar.

Notice that (8) and (13) provide a link between the algorithmic-level performance related to $\gamma$ and $\gamma_{\mathrm{bin}}$ with the system-level performance for a FMCW radar system with given set of specifications ($P_{\mathrm{t}}$, $G_{\mathrm{t}}$, $F$, *etc.*). To illustrate how this work, we present the following example of a typical 24 GHz FMCW radar for traffic monitoring applications. The specifications of the example radar system is shown in Table 1. We consider the detection of three types of targets, pedestrian, cyclists and cars. The average RCS for these targets are $1m^2$, $2m^2$ and $100m^2$ respectively [3]. We consider a Swerling I channel and use a CFAR detector [5] with a fixed FAR of 0.1%. The algorithmic-level performance for the CFAR detector is shown in Figure 4(a). It clearly indicates the achieved detection probability for different SNR ($\gamma$) values and the detection probability is consistent with the analytical results given by (13). Using (8) and (13), the system-level performance of the example FMCW radar is shown in Figure 4(b). This gives system designer a clear indication on the detection probability that can be achieved for different targets at different distances.

# 3 The proposed detector

A well know property of the FFT is that each frequency bin has a sinc-shaped spectrum [2]. When the beat frequency of the target falls exactly on the FFT grid, i.e. in the middle of a frequency bin, as shown in Figure 5(a), the FFT output has maximum signal amplitude (normalized to 1 in Figure 5(a)) and there is no leakage of the target signal to the other frequency bins. The performance of FMCW radar can be characterized with the model in Section 2. However, when the beat frequency of the target falls in between the FFT grids as shown in Figure 5(a) for the special case in which the beat frequency is in the middle of two FFT grids, we observe two detrimental effects. Firstly, the amplitude of the target signal at the FFT output is attenuated, which

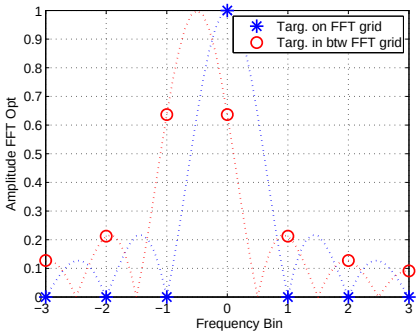


(a) Effects of FFT outputs when the target is not on the FFT grid.

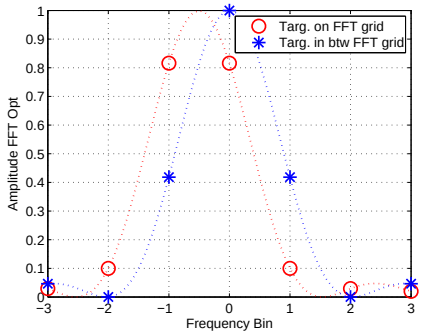


(b) Effects of FFT outputs using Hanning window when the target is not on the FFT grid.

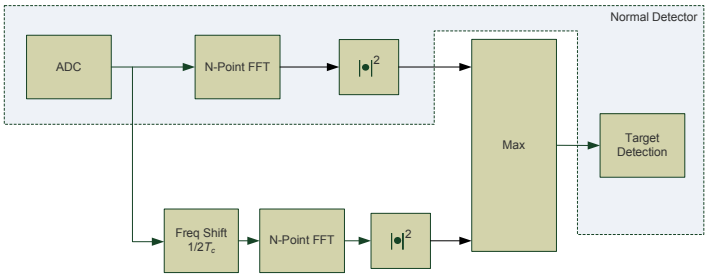


Figure 5: Proposed detector structure.

leads to degradation of the detection probability. Secondly, due to signal leakage, one target can produce multiple signals in different frequency bins. This increases the FAR in the other frequency bins. This degradation can be measured by the average FAR over all frequency bins. When the target is on the FFT grid, the average FAR is equal to the FAR per bin, as the noise in all the frequency bins has equal variance. When the target is not on the FFT grid, the FAR of neighbouring frequency bins of the target will increase significantly due to the signal leakage. As a result, the average FAR over all frequency bins also increases. It can be easily shown that the worst case happens when the target falls in the middle of two FFT grids, which leads to worst signal attenuation and largest leakage to other frequency bins. One popular approach to mitigate the signal attenuation and suppress the signal leakage due to high side-lobes of sinc function is to use a windowing function before FFT. Figure 5(b) shows the FFT output using a Hanning window for the same targets shown in Figure 5(a). We can see that using a hanning window, both signal attenuation and leakage are reduced for target in between two FFT grids. However, the frequency resolution of the FFT is reduced as the width of the main lobe is doubled.

In this paper, we propose a new detector that improves the detection probability for off the FFT grid targets without sacrificing frequency resolution. The proposed detector, as shown in Figure 5, includes a normal detector shown in the shaded box, which has good detection performance for targets on the FFT grid. We added a second branch to take care of the worst case in which the target is in the middle of two FFT grids. In this branch, a frequency shift of half a frequency bin ($1/2T_c$) is introduced before the FFT. In this way, the worst case target is shifted onto the FFT grid. Taking the maximum of the square law ($|\bullet|^2$) detector outputs from two branches, the output for a target in the middle of the two FFT grids is shown in Figure 6. Comparing this with the normal detector output, we can see that the amplitude of the target signal is increased, which leads to better detection probability. However, the signals leaked to other frequency bins still remain and thus the false alarm rate will not be improved.

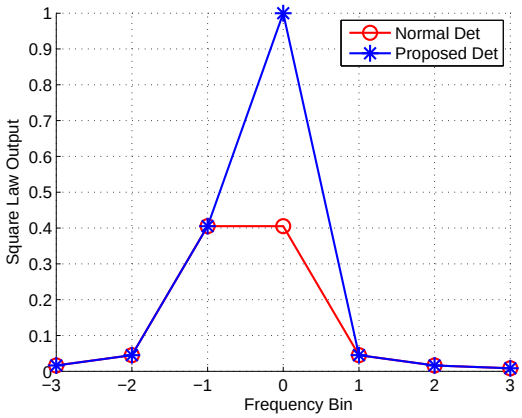


Figure 6: Output of the proposed detector when the target is in the middle of two FFT grids.

In fact, the average FAR over all the frequency bins will be degraded slightly. This is because the Max(•) operation selects the larger of the two noises at the two branches, hence, causes a slight increase in the average FAR.

# 4 Simulation Results

Computer simulations were used to study the performance of the proposed detector. Same as before, we assume a Swerling I channel [3] and use a constant false alarm rate (CFAR) detector [5] with a fixed false alarm rate (FAR) of 0.001. The decision on the presence of targets is made using only one chirp signal. Figure 7(a) shows detection probability when the target is on the FFT grid and when the target is in the middle of two FFT grids. When the target is in the middle of two FFT grids, due to signal attenuation, the detection probability performance is degraded by 3.9 dB ($= 20 \times \log_{10}[\text{sinc}(0.5)]$) as compared to the case when the target is on the FFT grid. The average FAR performance for the same two groups of targets is shown in Figure 7(b). When the target is on the FFT grid, the average FAR is equal to the per bin FAR of 0.001. However, for target in the middle of two FFT grid, due to signal leaking to other frequency bins, we observe a significant increase in the average FAR.

Figure 8(a) shows the performance of proposed detector for targets in the middle of the FFT grids. Compared to a normal detector, we observe a significant improvement on the detection probability. In fact, the detection probability is the same as when the target is on the FFT grid. The FAR performance of the proposed detector is shown in Figure 8(b). Consistent with the explanation in Section 3, there is a slight degradation in the FAR performance due to the Max(•)operation on the noise over the two branches in the proposed detector.

# 5 Conclusions

In this paper, we presented a system-level mathematical model that maps the signal to noise ratio (SNR) related detection algorithm performance to system-level detection performance for specific frequency modulated continuous wave (FMCW) radar systems. We also showed that normal FFT-based FMCW detector suffers degradation in terms of reduction in detection probability and increase in average false alarm rate (FAR), when the target is not on the FFT grid. We proposed a new detector, which by combining

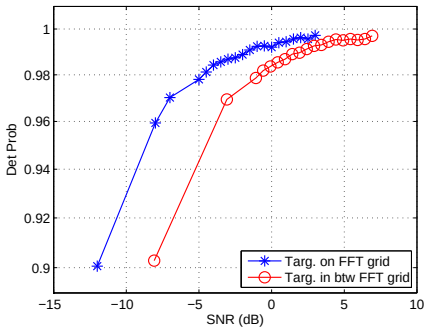


(a) Detection probability of CFAR detector for targets in the middle of the FFT grids.

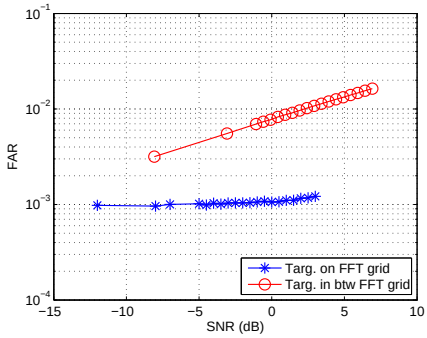


(b) Average FAR over all frequency bins of CFAR detector for targets in the middle of the FFT grids.

Figure 7: Detection probability and average FAR over frequency bins of FMCW radar for targets in the middle of the FFT grids.

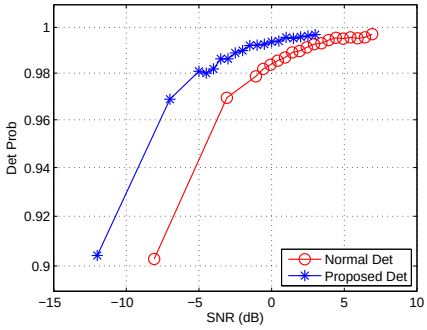


(a) Detection probability of the proposed detector for targets in the middle of the FFT grids.

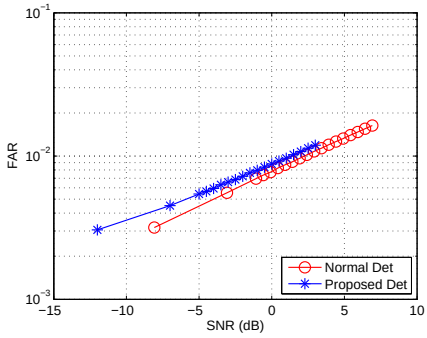


(b) FAR of the proposed detector for targets in the middle of the FFT grids.

Figure 8: Detection probability and FAR of the proposed detector for targets in the middle of the FFT grids.

the original FFT output with a frequency-shifted FFT output improves the detection probability significantly. However, the proposed detector has a slightly higher average FAR than the normal detector.

# References

[1] A. G. Stove, "Linear FMCW radar techniques," *IEE Proceedings F Radar and Signal Processing*, vol. 139, no. 5, pp. 343–350, 1992.

[2] A. V. Oppenheim, R. W. Schafer, and J. R. Buck, *Discrete-time signal processing*, 2nd ed. Prentice-Hall International, 1999.

[3] M. I. Skolnik, *Introduction to radar systems*, 3rd ed. Mc- Graw-Hill Ltd., 2001.

[4] G. M. Brooker, *Sensors for ranging and imaging.* SciTech Publishing, 2009.

[5] P. P. Gandhi and S. A. Kassam, "Analysis of cfar processors in homogeneous background," *IEEE Trans. Aerosp. Electron. Syst.*, vol. 24, no. 4, pp. 427–445, 1988.